Characterizing the Dynamic Behavior of Nano-TiO_2 Agglomerates in Suspensions by Photocorrelation Spectroscopy

I-Hsiang Tseng, Stephanie S. Watson, Li-Piin Sung

National Institute of Standards and Technology, 100 Bureau Dr Stop 8615 Gaithersburg MD 20899 USA

Abstract Metal oxide nanoparticles are small but easily form agglomerates in suspension, depending on the strength of particle-particle and particle-media interactions. To understand the agglomeration behavior of nanoparticles in media and relate to it to product performance testing, measurement methods are desired to characterize highly scattering metal oxide nanoparticle suspensions without dilution. In this paper, we describe the advantages of using photocorrelation spectroscopy (PCS) in a backscattering detection configuration to carry out a realistic agglomerate size measurement in multiple scattering media found in most metal oxide nanoparticle suspensions. The dynamic behavior of nano-titanium dioxide (TiO_2) particles in buffer solutions of different chemical composition and pH values was investigated as a sample system using PCS. The resulting autocorrelation functions (AF) at different time intervals, particle concentrations, and pH values were measured at several detection angles. The AF exhibits a multi-mode relaxation time feature and the calculated hydrodynamic diameters strongly depended on media composition and detection angle. This result indicates that the size and dispersion of nano-TiO_2 agglomerates are significantly affected by solution media. A measurement protocol for determining size and dispersion of metal oxide particles in media is proposed and related to a performance test found in industry.

Keywords: photocorrelation spectroscopy, nanoparticle, agglomerate, non-ergodic, TiO_2

Introduction Metal oxide particles have traditionally been used in a wide variety of applications, which include catalysis, sensors, semiconductor devices,

fuel cells, electrochemical batteries, paints, inks, and polymer composites. Recently, many innovative technical advances involving metal oxide nanoparticles have been made and commercialized, for example, incorporating metal oxide nanoparticles into polymer systems to improve UV and scratch resistance [Allen et al. 1998; Turton et al. 2001; Ammala et al. 2002]. From nanoparticle synthesis to final product preparation, the solution phase is involved in several processes. It is essential to characterize particle size and dispersion in solution for successful end-use applications.

Metal oxide nanoparticles are small but easily form micron-sized aggregates and/or agglomerates in suspension depending on the strength of particle-particle and particle-media interactions. Current methods used to characterize nanoparticle size in suspensions are often performed in dilute states; thus, results may not correlate to actual manufacturing processes and end-use performance. To understand the agglomeration behavior of nanoparticles in media and to relate it to performance testing in industry, measurement methods are desired to characterize highly scattering metal oxide nanoparticle suspensions without dilution. Continuing efforts have been made to explore alternative approaches to measure size and dispersion of highly scattering metal oxide nanoparticles in non-dilute states, but limitations still exist.

One practical and commercially available particle sizing technique is dynamic light scattering (DLS), which is also known as quasi-elastic light scattering (QELS) based on the photo correlation spectroscopy (PCS) technique. For most commercial DLS instruments, sample dilution is needed to avoid multiple scattering effects due to a fixed 90° angle of detection incident to the laser. For general research applications, a more versatile DLS measurement (referred to as PCS in the commercial DLS community) can be used. With a more flexible optical layout, the PCS technique has been used to investigate dynamic properties of proteins, polymers and nanoparticles by monitoring the time and angular dependence of the apparent diffusion coefficient (Georgalis et al., 1998; Chu et al., 2000; Rodriguez-Maldonado et al., 2005; Susoff et al., 2008). The hydrodynamic diameter (or apparent particle size) can then be estimated from the Stoke-Einstein equation assuming spherical particles in Brownian motion (Brant et al., 2005; Colomer et al., 2008; Das et al. 2008). This technique can easily be expanded to characterize the dynamic behavior and concentration dependence of

apparent particle size in semi-dilute suspensions (appearing slightly turbid visually).

Suspensions, such as those encountered in catalysis and coatings applications, have high particle concentrations with large agglomerate sizes and/or highly scattering particles with a high index of refraction. For these highly-diffuse, turbid suspensions, multiple scattering dominates. In this case, the light scattered by one particle is in turn scattered by other particles prior to arriving at the detector. The scattering signal-to-noise ratio is greatly reduced by multiple scattering in the forward direction. The resultant photon correlation function and deduced apparent particle sizes are highly dependent on the detection angle. To obtain meaningful size information, PCS measurements, with a modified optical design using a backscattering detector configuration, are often used to decrease the effect of multiple scattering on photon detection (Kaszuba et al., 2006; Kaszuba et al., 2007).

In this paper, we explore the advantages of using multiple angle PCS to measure agglomerate size in non-dilute nano-titanium dioxide (TiO_2) particle suspensions and investigate the dynamic agglomeration behavior of nano-TiO_2 particles in various solution media. In additional to multiple scattering, other key parameters, such as particle-particle and particle-media interactions, will be investigated using spectrophotometric assay suspensions commonly used in industry to measure photoreactivity in TiO_2. These assay suspensions utilize buffer systems with different chemical compositions, pH values, and different dyes, all of which vary the strength of the particle-particle interactions in the solutions. The effect of particle size and agglomeration resulting from buffer composition and pH value and its relationship to TiO_2 photoreactivity response determined from the industrial assays will be described in more detail in a forthcoming paper. In this study, PCS measurements were performed at various scattering angles and different time sequences for selected particle concentrations to study the size, dispersion, and agglomeration development in nano-TiO_2 particles. The resulting autocorrelation function (AF) was analyzed using a non-linear least square (NLLS) fit to determine the apparent hydrodynamic diameter of agglomerates in solution and to determine if the size and dispersion of nano-TiO_2 agglomerates are significantly affected by the media environment. Finally, an in-

situ measurement protocol is proposed to measure the size of agglomerates, their stability in suspensions, and agglomeration kinetics.

Experimental*

Materials and Sample Preparation Polystyrene (PS) size standards in suspension (NIST traceable Standard Reference Materials, nominal sizes: 60 nm, 304 nm and 800 nm; Duke Scientific Corp.) were used as calibration references. Commercial TiO_2 nanoparticles with a primary crystallite particle size of 25 nm were suspended in aqueous methyl viologen (MV) spectrophotometric assay components as described in a previous study (Watson S, et al. 2008). Briefly, a TiO_2 suspension was prepared with methyl viologen dichloride and disodium ethylenediaminetetraacetic acid (EDTA) adjusted to pH = 6.0 with a phosphate buffer. In other MV assay experiments, a potassium hydrogen phthalate (KHP) buffer was used to eliminate phosphates in solution. The TiO_2 suspension, purged in argon (Ar), was then irradiated with ultraviolet (UV) radiation and transferred to a cuvette for UV-visible (UV-VIS) spectroscopy. Designated buffer composition and pH value labels are listed in Table 1. Each sample was prepared by mixing the nanoparticle with a specific assay buffer solution, which was filtered through a 0.45 μm filter (Whatman) to remove large dust particles. A 15-min ultrasonication procedure using a mechanical ultrasonic cleaner (Fisher Scientific, FS20) was applied to each prepared sample prior to each PCS measurement. Because the solution environment critically affects the size of nanoparticle agglomerates, PCS measurements were conducted immediately to characterize the dimension of nano-TiO_2 agglomerates in aqueous photoreactivity assay solutions without further dilution. For comparison, samples of dilutions from the initial photoreactivity assay solution were also measured to examine how the size of nano-TiO_2 agglomerates and the state of particle dispersion in solution change due to dilution.

* Certain trade names and company products are mentioned in the text or identified in an illustration in order to adequately specify the experimental procedure and equipment used. In no case does such an identification imply recommendation or endorsement by the National Institute of Standards and Technology, nor does it imply that the products are necessarily the best available for the purpose.

Measurement Technique

Photo Correlation Spectroscopy (PCS) PCS measurements were performed using a variable angle light scattering instrument (Scitech Instruments, Inc.) with a 45 mW Nd:YAG laser having a wavelength of 532 nm. This instrument utilized a compact optical fiber system that was designed for laser delivery, scattered light collection, and transmitted beam collection. Dual photomultiplier tubes (PMT) and amplifiers are used for measurement and cross-correlation of detected light. A correlator with a minimum lag time of 11.6 ns and 288 pseudo-logarithmically spaced channels is also included in the instrument configuration. A cylindrical sample cell of diameter of 15 mm (Wheaton Vial File) was placed in a sample holder that consisted of a temperature-controlled circulating oil bath at 25 ^{o}C. For angular-dependent experiments, the AF was acquired at scattering angles of 15^{o}, 30^{o}, 90^{o}, 120^{o}, 150^{o}, 173^{o} for 1 min to 30 min. Prior to measurement at a different angle, the sample was sonicated for 15 min to redisperse the nanoparticles. Time-dependent experiments were conducted at a scattering angle of 173^{o} at one-min time intervals for a period of 30 min without disturbing the samples.

PCS Data Analysis The intensity autocorrelation function, $g^{(2)}(\tau)$, obtained from PCS measurements is directly related to the electric field autocorrelation, $g^{(1)}(\tau)$, by applying the Siegert equation (Frisken, 2001) for single-mode optical fibers in the detector optics, as shown in Equation (1):

$$g^{(2)}(\tau) = 1 + [g^{(1)}(\tau)]^2 \tag{1}$$

For mono-dispersed particles in solution, the normalized field autocorrelation $g^{(1)}(\tau)$ is characterized by a single exponential decay equation,

$$g^{(1)}(\tau) = A\exp[-\Gamma\tau] \tag{2}$$

with a decay rate (Γ) or relaxation time ($1/\Gamma$) where,

$$\Gamma = Dq^2 \tag{3}$$

D is the translational diffusion coefficient, which is associated with temperature (T), Boltzmann constant (k_B), viscosity of solvent (η), as well as the hydrodynamic radius of particles (R_h) as in the Stoke-Einstein relation:

$$D = \frac{k_B T}{6\pi\eta R_h} \tag{4}$$

q is the scattering vector, which is related to the scattering angle (θ), wavelength of incident light (λ_o) and the index refraction of solvent (n_o) by the following equation

$$q = \frac{4\pi n_o \sin(\theta/2)}{\lambda_o} \tag{5}$$

The field autocorrelation function $g^{(1)}(\tau)$ can be further defined with the following equations for mono-dispersed spherical particles in suspension.

$$\begin{aligned} g^{(1)}(\tau) &= \sqrt{g^{(2)} - 1} \\ &= A\exp[-(\frac{k_B T}{6\pi\eta R_h}) * [\frac{4\pi n_o \sin(\theta/2)}{\lambda_o}]^2 \tau] \end{aligned} \tag{6}$$

The value of the characteristic decay rate (Γ) can be obtained using a non-linear least square (NLLS) fit to Equation 6. The diffusion coefficient (D) and the hydrodynamic diameter ($2R_h$) based on Stoke-Einstein relation (Eq. 4) can also be determined. Values of the parameters used in this study are listed in Table 2.

As mentioned above, the autocorrelation function of monodispersed particles in solution can be characterized by the single exponential decay equation (Eq. 6). For a non-monodispersed system, a combination of exponential decay functions, such as a bimodal exponential function shown in Eq. 7 was used.

$$\begin{aligned} g^{(1)}(\tau) &= A_o + A_1 \exp[-\Gamma_1 \tau] + A_2 \exp[-\Gamma_2 \tau] \\ &= A_o + A_1 \exp[-D_1 q^2 \tau] + A_2 \exp[-D_2 q^2 \tau] \end{aligned} \tag{7}$$

Multi-mode decay rates (Γ_i) and the corresponding proportion (A_i) of particles with a specific size can be estimated from normalized $g^{(1)}(\tau)$ by NLLS fitting. The apparent particle size ($2R_h$) associated from each diffusion coefficient, D_i, is calculated. For most systems examined in the study, a bimodal fitting routine worked successfully. However, more decay rates, D_1 to D_5, were needed to obtain a better fitting result and size distribution plot for some polydispersed particle suspensions.

Results and Discussion

The apparent size of particles in suspension can be determined by analyzing the AF obtained from each sample. In order to explore its angular dependence, the AF of each sample was acquired at different scattering angles ranging from 15^o to 173^o. Figure 1 illustrates a series of experimental AFs for the PS size reference

standard of nominal diameter of 300 nm at different scattering angles. The AF at each angle presents a characteristic decay rate or relaxation time, which is related to the scattering vector as shown in equation 3. Figure 2(a) shows the linear relationship of the decay rate (Γ) for this PS standard sample (300 nm) to the square of the scattering vector (q), thus, as shown in Figure 1, the characteristic relaxation time (or decay time) shifts toward a shorter lag time when the scattering angle increases. Evaluation of the AF at different angles for this PS standard gives the same apparent particle size, as shown by the flat line in Figure 2(b). This non-angular dependence indicates the monodispersed particles size and lack of multiple scattering in this sample. The details of analyzing the AF are described in the next section.

Figure 3 illustrates the experimental AFs (open symbols) and fitted curves (solid lines) for three PS size reference standards with a nominal diameter of 60 nm, 300 nm and 800 nm at a scattering angle of 173°. Each PS size standard shows a different AF curve. The decay curve for the 60 nm reference standard features a faster decay rate (Γ), i.e. shorter characteristic decay time than that for the 300 nm or 800 nm reference standard. The curve for the 60 nm reference standard starts to decay monotonically around 0.1 ms based on a NLLS fitting to a single (or mono-) exponential decay function. The characteristic decay times for the 300 nm and 800 nm reference standards are around 0.6 ms and 1.8 ms, respectively. The goodness of the fit also indicates the monodisperse feature of the PS size standards. Based on Eq. 4, the calculated hydrodynamic diameters ($2R_h$) for the three PS standard size samples are (67 ± 1) nm, (304 ± 4) nm and (838 ± 20) nm, which is within uncertainties of the reported NIST traceable SRM values: (59 ± 9.9) nm, (300 ± 5.1) nm and (799 ± 8.3) nm. The uncertainty values in the measurements represent the standard deviation from the mean value.

For most realistic suspensions, however, the nanoparticle agglomerates possess a range of dimensions, and the resultant AFs cannot be fitted perfectly to a single exponential decay curve as shown in Figure 1. Figure 4 displays such an example of a measured AF (open circles) from a commercial nanosized TiO_2 sample in P6 media (1 g/L) at 173°. Several fitting routines, based on Eq. 6 and 7, were used to determine the best fit of the data. It is clear that the experimental data is best fitted by a sum of the two exponential functions (solid line) rather than by a single exponential curve (dotted line), which was used for the PS reference

standard samples. The dotted single exponential curve only partially fits the experimental data, and an average hydrodynamic diameter of (934 ± 16) nm is obtained. The bimodal function provides a better fit for the experimental data. The fitted results show equal amounts of two agglomerate diameters, (500 ± 58) nm and (1,680 ± 180) nm. The size of both agglomerates is much larger than the assumed primary size of nano-TiO_2 (~ 25 nm) and is an indication of the degree of agglomeration of nanoparticles in the suspensions.

The AFs from Figures 1, 3 and 4 exhibit a characteristic ergodic system, in which the AF decays to nearly zero at long lag times. However, some samples show gel-like, non-ergodic behavior, where the AF decays to a non-zero plateau value (Ozon et al. 2006). Figure 5 shows an example of such an AF with two distinguishable relaxation modes - slow and fast modes. In this case, the sample consists of nanosize TiO_2 particles in P6 suspension at a higher TiO_2 concentration (5 g/L). The obtained non-ergodic AF can be fitted by separating the time before the plateau (fast-mode section) from the time after the plateau (slow-mode section) or by using the entire curve with a summation of exponential decay curves. For the fast-mode section, a bimodal exponential fitting was selected to fit the first segment of data. The result for the fast-mode decay curve shows 94 % contribution from agglomerates with a diameter of (910 ± 50) nm and 6 % from (100 ± 10) nm particles. The slow-mode section of the AF is the result of a gel-like macron (> 10 μm) network structure due to agglomeration. Similar non-ergodic behavior was also observed for other high concentration nanoparticle suspensions at different pHs and photoreactivity assay media.

As mentioned previously, the decay rates (Γ) deduced from the AF data from PCS measurements can provide size information on agglomerates in the suspensions. However, the decay rate varies with the various scattering angles due to the different probing size scale. For a self-diffuse system (often a dilute solution), the measured Γ is proportional to the square of wave vector (q^2), i.e. $\Gamma = Dq^2$ (eq. 3). Thus the system has a unique self-diffusion coefficient, D, and a well-defined particle size, R_h, using eq. 4 assuming a spherical shaped particle. If the decay rate does not follow the self-diffusion equation, eq. 3, the angular dependence of the decay rate is often used to analyze the particle shape/structure information (Badaire et al. 2004; Georgalis et al. 1998, Ozon et al. 2006, Witten et al. 2008) as well as serve as an indication for multiple scattering. To evaluate the

angular dependence of the PCS data and further determine the accuracy of the particle size measurements at any scattering angle, a series of PCS experiments were conducted at various scattering angles ranging from 15° to 173° for the particle suspensions at different concentrations.

Figure 2a displays the decay rate (Γ) as a function of q^2 for the PS size standards (60 nm and 300 nm) in water and TiO_2 particles suspended in P6 media at two different particle concentrations, 1 g/L (TiO_2 /P6 (1)) and 0.1 g/L (TiO_2 /P6 (0.1)), respectively. The Γ values were extracted from the AFs fitted by a single exponential decay function at different scattering angles. Figure 2b presents the calculated particle size from each decay rate in Figure 2a as a function of the corresponding scattering angle. As expected, the Γ values for the PS size standards are proportional to the square of wave vector (q^2), as shown in the linear fit of the data in Figure 2a. The corresponding apparent particle diameter (in Figure 2b) is independent of scattering angle. However, for the TiO_2/P6 (0.1) sample, the data deviates from the linear progression. The corresponding calculated diameters of TiO_2/P6 (0.1) are no longer independent of scattering angle. A larger particle size was obtained at angles larger than 90^o with large measurement uncertainties. The large measurement uncertainties are due to a poor fit to a single exponential decay function. This result reflects the polydispersity of TiO_2 particles in a realistic assay system. Notably, the calculated particle sizes are smaller in the forward scattering direction than in the backscattering direction. This observation is consistent with results found in the presence of the multiple scattering (Kaszuba et al. 2007).

It is expected that the impact of multiple scattering on the particle size measurements will be more pronounced for suspensions with higher TiO_2 concentrations. Indeed, for a higher particle concentration sample, TiO_2/P6 (1), the relationship between Γ and q^2 follows a completely different trend. In this case, the transmission of the sample (through 15 mm cell) was only 20 % and the sample appeared turbid. Furthermore, the scattered intensity at smaller angles (in the forward scattering direction) is lower than at larger angles (in the back scattering direction). Consequently, smaller values of Γ are observed at larger scattering angles, and the apparent particle size of TiO_2/P6 (1) dramatically decreases with decreasing scattering angle. The apparent size deduced from PCS

measurements at 173^o is around 500 nm but it was 100 times smaller at the angles less than 30^o. Note that this deduced size is smaller than the primary particle size of nano-TiO_2 particle, 25 nm, obtained from the manufacturer. Again, this observation is an indication of the effect of multiple scattering, which would result in unreasonable calculated particle sizes at small scattering angles.

For systems with high particle concentrations, the multiple scattering effects can be eliminated by sample dilution or reduced using a backscattering detection configuration to obtain true particle size information. For our study, the chosen concentration of 1 g/L is that used in industrial photoreactivity assay measurements and so to obtain realistic particle agglomerate size information without dilution, the PCS measurement with a backscattering configuration is preferred. Note that although this particular concentration of nanoparticles is not truly considered highly concentrated based on particle volume concentration calculations, the TiO_2 is highly scattering due to its index of refraction. The Γ values or the calculated sizes from an optimum backscattering angle, in this case at 173^o, provide true size information. This assumption is confirmed in both plots in Figure 2, where the two concentrations (0.1 g/L and 1 g/L) of TiO_2/P6 samples had almost identical values in Γ and calculated particle diameters, within measurement uncertainties, at a scattering angle of 173^o. Optimization of the appropriate scattering angle in relation to signal to noise must be performed for each nanoparticle suspension. Similar results were obtained for the same nanosize TiO_2 and other nanoparticles in the other MV photoreactivity assay conditions (such as in KHP buffer). This result provides insights into the measurement of turbid, highly scattering samples using PCS in the backscattering detection configuration.

In addition to the multiple scattering problems, one other challenge encountered in measuring particle size in the photoreactivity assay systems is the stability of the suspensions. This type of suspension is often unstable and particles settle after a short period of time. To measure particle size and the dynamics of the agglomeration process before sedimentation, a short-duration PCS measurement is required. It has been suggested that the backscatter detection method increases the sensitivity of instrument as well as the detection limit for particle/agglomerate size and concentration (Kaszuba et al., 2006-2008). Furthermore, backscattering detection minimizes the probability of multiple

scattering as well as results in a higher intensity with a longer decay rate of the intensity fluctuation. These features enable short-duration measurements with good statistics for non-dilute, highly scattering suspensions, such as the photoreactivity assay suspensions. For example, in this study the scattering intensity at 173^o was more stable than that obtained from other angles below 90^o, and the stability of the AF was long enough to obtain a good short-duration measurement with reliable results.

Figure 6 shows the AFs determined from PCS at 173^o for TiO_2/K6 (1) system at different time intervals immediately after placing the samples in the light scattering instrument. Clearly, the turn-over of the AF curve (or the decay time) moves toward a longer lag time and a slow-mode plateau is formed as a function of time in the instrument without disturbing the suspension. Using NLLS fitting (not shown), a broadened decay curve instead of single exponential decay resulted, a sign that the TiO_2 particles are undergoing a fast process of agglomeration with a broad particle size distribution. The changes in the dynamic behavior of TiO_2 suspensions were examined by analyzing the AFs collected every minute for a final time of 30 min, such that each AF represents the average behavior within one minute of the measurement time. A bimodal exponential decay function was used to fit these AFs, and the calculated apparent diameter of the primary TiO_2 agglomerates at each time point is shown in Figure 7 for the two MV buffers at two pH values, as indicated in the legend. In the KHP buffer (K, square symbols), the primary particle size of the TiO_2 particles changes rapidly with measurement time. Within the initial 5-min measurement time, the TiO_2 agglomerates in the K6 system (pH = 6) appear to have a size around 1 μm, and increase to almost 5 μm in 30 min. In the K4 system (pH = 4), the growth rate of the particle size is similar to the K6 system with a slightly smaller size (around 4 μm). On the other hand, much slower growth of TiO_2 agglomerates was observed in the phosphate buffer (P, triangle symbols). The final apparent particle size in the P6 system (pH = 6) is around 800 nm, which is nearly twice the initial particle/agglomerate size, but is much smaller than in the KHP system. Similar trends in the time-dependent growth of TiO_2 agglomerates are observed for the low pH value in the phosphate system with a lower final particle diameter in the period of 30 min. This result reveals the importance of time-dependent studies and provides insights into the stability of particles in various solutions. A detailed

report on the effects of buffer composition and pH value on changes in nano-TiO_2 particle size and agglomeration rate and its relationship with photoreactivity response for industrial assay measurements will be given in an upcoming paper.

Concluding Remarks

PCS measurements have been used to determine the size of nano-TiO_2 agglomerates in suspensions containing different buffer conditions and particle concentrations. The corresponding AFs at various scattering angles and time intervals were analyzed using NLLS curve fitting to a single or multi-mode exponential function. The deduced decay rates and particle sizes in different environmental conditions were used to determine and justify a best practice for the measurements. For the highly scattering and realistic concentrations of TiO_2 particles in suspensions (such as photoreactivity assays) studied without further dilution, the PCS measurement with a backscattering detection is best used to eliminate the effect of multiple scattering, which often underestimates the particle size. Additionally, backscattering detection also provides a means to study the dynamics of particle agglomeration using a series of short-duration PCS measurement.

Based on this study, a measurement protocol using the PCS technique to measure the stability of nanoparticles in suspensions and to determine meaningful particle size in a realistic non-dilute particle suspension can be established as follows:

1. Evaluate as-received samples by observation of the turbidity in the sample or inspection of its transmission to determine if the sample is highly scattering, i.e. the transmission is below 50 % or absorbs laser light (not visually transparent).
2. Check the stability of fluctuation and the intensity of scattering light intensity (I_{scatt}) at several angles. If I_{scatt} at back scattering angles is greater than that at forward angles, use a backscatter detection method and determine an optimum scattering angle with the best stability and statistics to obtain meaningful size estimations.
3. Verify the instrument performance by examining reference samples, such as the PS size standard used in this study.
4. For determination of an apparent size of particles in a suspension, conduct a PCS measurement to obtain a representative AF for each sample. The

recording time for the AF should be adjusted to accommodate sample stability, instrument operating requirements, and data statistics. A minimum measurement time of 60 s is recommended for nanoparticle suspensions. A longer recording time (~ 30 min) can be applied for weakly scattering samples if a static sample is stable.

5. For dynamic or stability measurements, conduct the PCS measurements by recording the AF at short time intervals, such as every minute, depending on the data statistics, over a period of time.
6. After a representative AF is obtained, perform data analysis. Based on the theories and equations mentioned in the experimental section, normalize the obtained AF and use a non-linear least square fitting routine to extract size information, checking for the correct constants and units in each parameter. Fit the AF starting with a single-exponential decay curve. If the experiment data deviates from this regression curve, use a bimodal or multi-mode exponential decay function to acquire the most accurate and precise size information.

References

Ammala A; Hill AJ; Meakin P; Pas SJ; Turney TW; 2002, Degradation studies of polyolefins incorporating transparent nanoparticulate zinc oxide UV stabilizers, J of Nanoparticle Research 4: 167-174.

Allen NS; Edge M; Corrales T; Childs A; Liauw CM; Catalina F; Peinado C; Minihan A; Aldcroft D; 1998, Ageing and stabilisation of filled polymers: an overview, Polymer Degradation and Stability 61: 183-199.

Badaire S., Poulin P., Maugey M., Zakri C., 2004, In situ measurements of nanotube dimensions in suspensions by depolarized dynamic light scattering, Langmuir 20, 10367-10370.

Brant J., Lecoanet H., Wiesner M. R., 2005, Aggregation and deposition characteristics of fullerene nanoparticles in aqueous systems, J of Nanoparticle Research, 7: 545-553.

Chu B., Liu T., 2000, Characterization of nanoparticles by scattering technique, J of Nanoparticle Research 2: 29-41.

Colomer M. T., Guzman J., Moreno R., 2008, Determination of peptization time of particulate sols using optical techniques: Titania as a case study, Chem. Mater., 20: 4161-4165.

Das P, Mallick A, Sarkar D, Chattopadhyay N, 2008, Probe-induced self-aggregation of gamma-cyclodextrin: Formation of extended nanotubular suprastructure, J of physical chemistry C 112(26): 9600-9603.

Dhadwal H. S., 2007, Homodyne fiber optic backscatter dynamic light scattering, Optics Letters 32(23): 3391-3393.

Frisken B, 2001, Appl. Opt. 40, 4087-4091.

Georgalis Y., Starikov E. B., Hollenbach B., Lurz R., Scherzinger E., Saenger W., Lehrach H., Wanker E. E., 1998, Proc. Natl. Acad. Sci. 95, 6118-6121.

Kaszuba M., 1999, J. Nanopart. Res. 1, 405-409.

Kaszuba M., Connah M. T., 2006, Protein and nanoparticle characterisation using light scattering techniques, Part. Part. Syst. Charact. 23, 193-196.

Kaszuba M., Connah M. T., McNeil-Watson F. K., Nobbmann U., 2007, Resolving concentrated particle size mixtures using dynamic light scattering, Part. Part. Syst. Charact. 24, 159-162.

Kaszuba M., McKnight D., Connah M. T., McNeil-Watson F. K., Nobbmann U., 2008, J. Nanopart. Res. 10, 823-829.

Kelarakis A., Castelletto V., Krysmann M. J., Havredaki V., Viras K., Hamley I. W., 2008, Langmuir 24, 3767-3772.

Ozon F., Petekidis G., Vlassopoulos D., 2006, Signatures of nonergodicity transition in a soft colloidal system, Ing. Eng. Chem. Res. 45, 6946-6952.

Rodriguez-Maldonado L., Fernandez-Nieves A., Fernandez-Barbero A., 2005, Dynamic light scattering from high molecular weight poly-L-lysine molecules, Colloids and Surfaces A: Physicochem. Eng. Aspects 207-271: 335-339.

Susoff M., Winter D., Eisenbach C. D., Oppermann W., 2008, J. Phys. Chem. B, 112, 4519-4525.

Turton TJ; White JR, 2001, Effect of stabilizer and pigment on photo-degradation depth profiles in polypropylene, Polymer Degradation and Stability 74: 559-568.

Watson S., Forester A., Tseng IH, Sung L., “Assessment of Spectrophotometric Assay Methods on Nanostructured Pigments,” *ACS Symposium Series Book on "Nanotechnology Applications in Coatings,"* Fernando RH and Sung LP (eds.), Oxford University press, 2008.

Witten K.G., Bretschneider J. C., Eckert T., Richtering W, Simon U., 2008, Assembly of DNA-functionalized gold nanoparticles studied by UV/Vis-spectroscopy and dynamic light scattering, Phys. Chem. Chem. Phys. 10, 1870-1875.

Table 1 Parameters and Labels for the Methyl Viologen (MV) Photoreactivity Assay Matrix

Buffer Solution	pH	Label
Phosphate	6.0	P6
	4.4	P4
Potassium Hydrogen Phthalate (KHP)	6.0	K6
	4.4	K4

Table 2 Parameters used in Autocorrelation Function Curve Fitting Equations

Parameters	Symbol	Value	Unit
Wavelength of Laser	λ_o	5.34E-9	m
Index of refraction of solvent (H_2O) @ 25°C	n_o	1.333	-
Temperature	T	298	K
Boltzmann constant	k_B	1.3807E-23	$J*K^{-1}$
Viscosity of solvent (H_2O) @ 25°C	η	8.91E-4	Pa*s

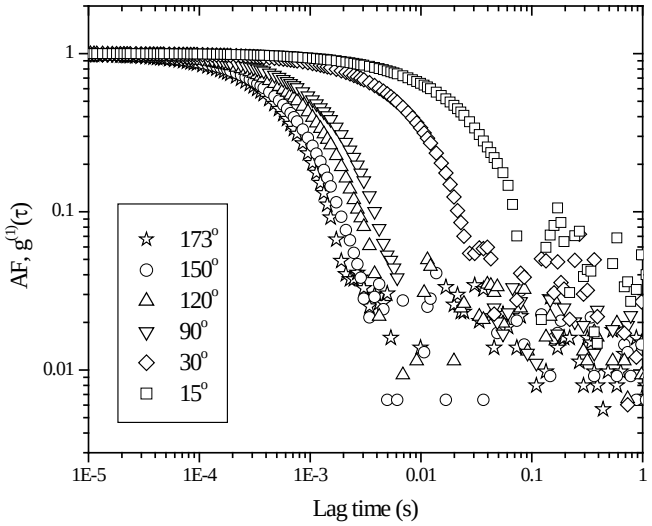

Figure 1 Normalized autocorrelation function (AF) measured at different angles between 15° to 173° for the polystyrene size reference standard (nominal size = 300 nm).

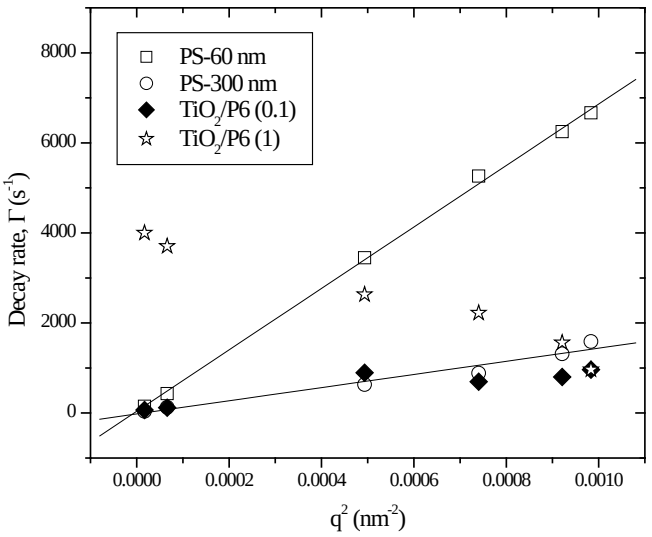

(a)

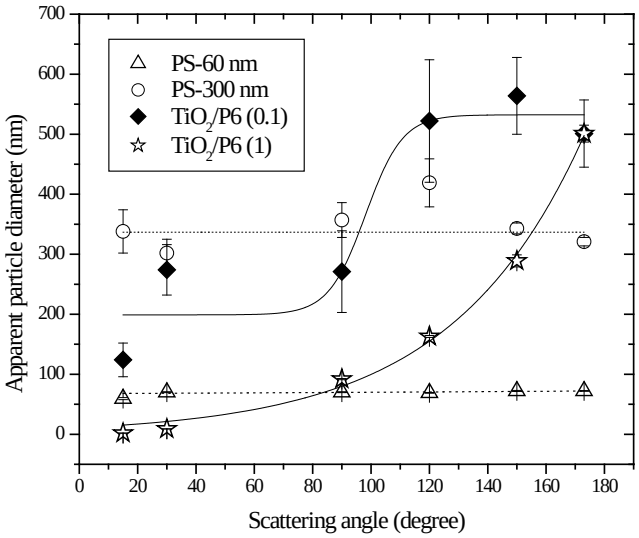

(b)

Figure 2 (a) Dependence of decay rate (Γ) with q^2 using decay times extracted from the fitting of autocorrelation functions obtained from various scattering angles for reference standards and TiO_2/P6 samples. (b) Angular dependence of calculated apparent diameter of size standards (60 nm and 300 nm) and TiO_2 in MV solutions (phosphate buffer, pH 6) at two concentrations, 1g/L (1) and 0.1 g/L (0.1). The error bar represents the standard deviation of each obtained data point. The lines shown in both graphs represent the regression results.

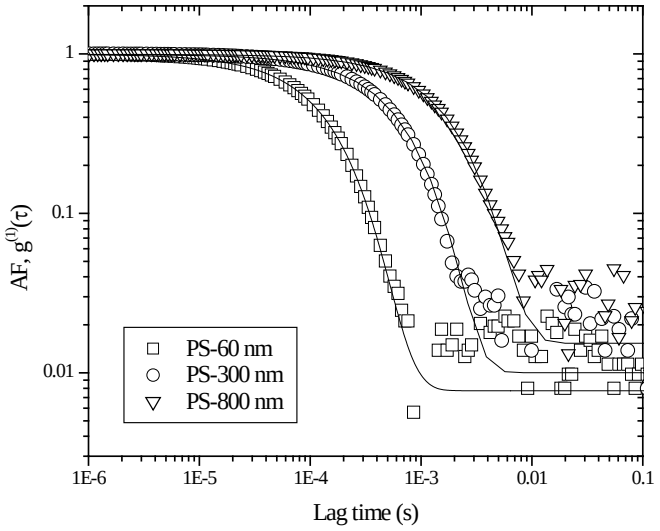

Figure 3 Normalized autocorrelation function (AF) measured at 173^{o} for polystyrene size reference standards (symbols). The solid lines show the fitting results of experimental data.

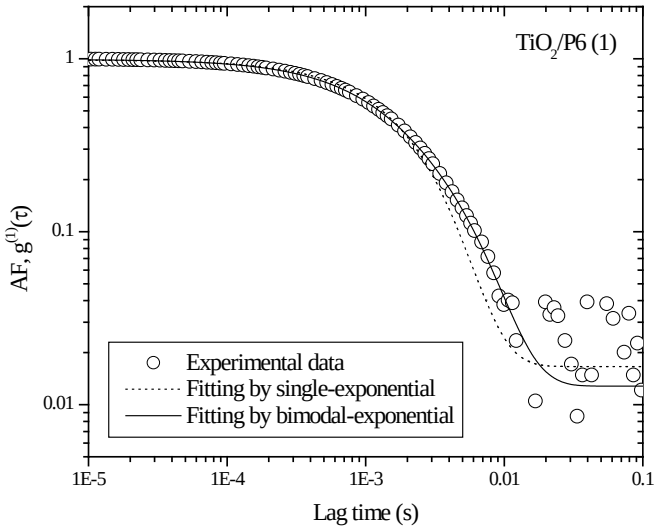

Figure 4 Normalized autocorrelation function (AF) measured at 173^{o} for TiO_2 in MV solution (phosphate buffer, pH 6, 1 g/L) and two curve fitting results as indicated in solid and dotted lines.

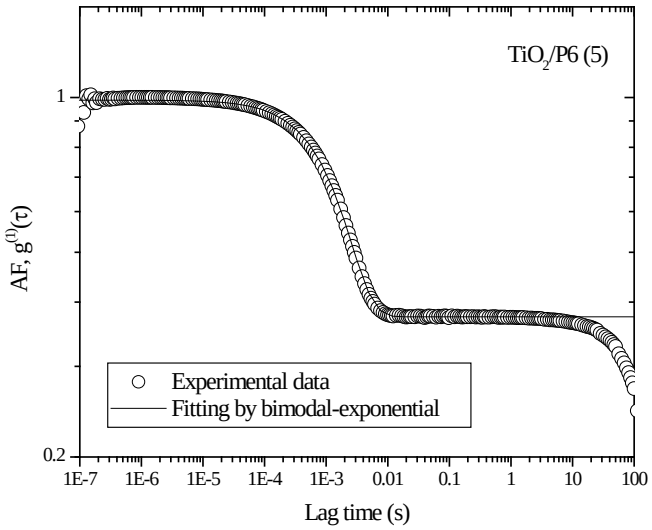

Figure 5 Normalized autocorrelation function (AF) measured at 173^o for concentrated TiO_2 in MV solution (phosphate buffer, pH 6, 5 g/L) and curve fitting result as indicated in solid line.

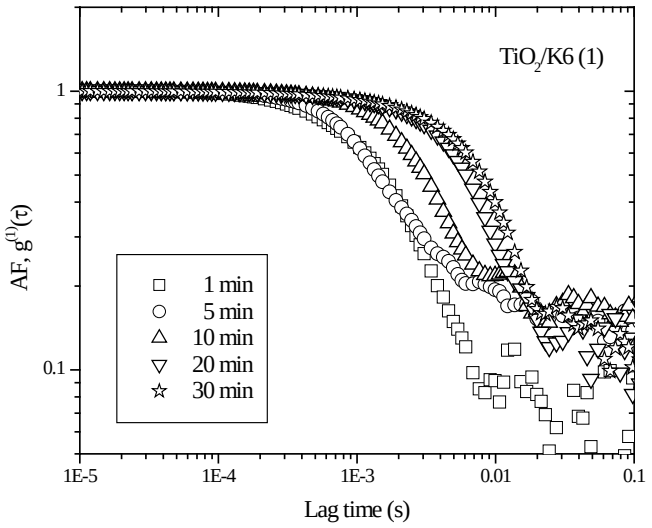

Figure 6 Time dependence of autocorrelation function (AF) measured at 173^o for TiO_2 in MV solution (KHP buffer, pH 6, 1 g/L).

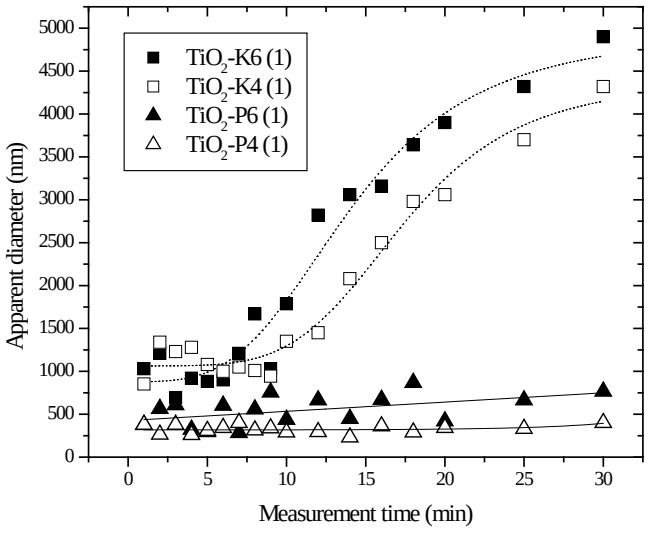

Figure 7 Time dependence of calculated apparent diameter of TiO_2 particles suspended in different MV solutions: phosphate (P) or KHP (K) buffer; pH value 4 or 6. TiO_2 concentration in each sample is 1 g/L. The lines represent the regression results.